PNAS
www.pnas.org

Supplementary Information for

Simple Framework for Constructing Functional Spiking Recurrent Neural Networks

Robert Kim, Yinghao Li and Terrence J. Sejnowski

Correspondence should be addressed to R.K. (rkim@salk.edu) or T.J.S. (terry@salk.edu).

This PDF file includes:

Supplementary text
Figs. S1 to S7
Table S1
References for SI reference citations

www.pnas.org/cgi/doi/10.1073/pnas.1905926116

Supporting Information Text

Implementation of computational tasks and figure details. In this section, we describe the details of the parameters and methods used to generate all the main figures in the present study.

Fig. 1. A rate RNN of $N = 200$ units (169 excitatory and 31 inhibitory units) was trained to perform the Go-NoGo task for Fig. 1B. Each trial lasted for 1000 ms (200 time steps with 5 ms step size). The minimum and the maximum synaptic decay time constants were set to 20 ms and 50 ms, respectively. An input stimulus with a pulse 125 ms in duration was given for a Go trial, while no input stimulus was given for a NoGo trial. The network was trained to produce an output signal approaching $+1$ after the stimulus offset for a Go trial. For a NoGo trial, the network was trained to maintain its output at zero. A trial was considered correct if the maximum output signal during the response window was above 0.7 for the Go trial type. For a NoGo trial, if the maximum response value was less than 0.3, the trial was considered correct. For training, 6000 trials were randomly generated, and the model performance was evaluated after every 100 trials. Training was terminated when the loss function value fell below 7 and the task performance reached at least 95%. The termination criteria were usually met at or before 2000 trials for this task.

For Fig. 1C, rate RNNs with 9 different sizes ($N = 10, 50, 100, 150, 200, 250, 300, 350, 400$) were trained. For each network size, 100 rate RNNs with random initial conditions were trained on the Go-NoGo task.

Fig. 2. The rate RNN trained in Fig. 1B was converted to a LIF RNN using different scaling factor (λ) values for Fig. 2B. The double exponential synaptic filter was used, and the gain term (g) for the rate RNN initialization was set to 1.5. The LIF parameters listed in Table S1 were used for all the LIF network models constructed in Fig. 2.

Fig. 3. Rate RNNs with 11 different network sizes ($N = 10, 50, 100, 150, 200, 250, 300, 350, 400, 450, 500$) were trained on the contextual integration task. For each network size, 100 rate RNNs with random initial conditions were trained.

For the task design, the input matrix ($\boldsymbol{u} \in \mathbb{R}^{4\times 500}$) contained four stimuli channels across time (500 time steps with 5 ms step size). The first two channels corresponded to the modality 1 and modality 2 noisy input signals. These signals were modeled as white-noise signals (sampled from the standard normal distribution) with constant offset terms. The sign of the offset term modeled the evidence toward (+) or (-) choices, while the magnitude of the offset determined the strength of the evidence. The noisy signals were only present during the stimulus window (250 ms – 1250 ms). The last two channels of $\boldsymbol{u}$ represented the modality 1 and the modality 2 context signals. For instance, the third channel of $\boldsymbol{u}$ is set to one and the fourth channel is set to zero throughout the trial duration to model Modality 1 context.

For each trial used to train the rate model, the offset values for the two modality input signals were randomly set to -0.5 or +0.5. The context signals were randomly set such that either modality 1 (third input channel is set to 1) or modality 2 (fourth input channel is set to 1) was cued for each trial. If the offset term of the cued modality was +0.5 (or -0.5) for a given trial, the network was instructed to produce an output signal approaching +1 (or -1) after the stimulus window. The model performance was assessed after every 100 training trials, and the training termination conditions were same as the ones used for Fig. 1.

Fig. 4. A network of $N = 250$ LIF units (188 excitatory and 62 inhibitory units) were constructed from a rate RNN model trained to perform the context-dependent input integration task for Fig. 4A. The scaling factor (λ) was set to 1/60. The double exponential synaptic filter was used, and the gain term (g) for the rate RNN initialization was set to 1.5. The LIF parameters listed in Table S1 were used for all the LIF network models constructed in Fig. 4.

Fig. 5. Rate RNNs ($N = 250$) were trained on the Go-NoGo task with and without optimizing the synaptic decay time constants ($\boldsymbol{\tau^d}$). For each condition, 100 rate RNNs were trained. For the fixed synaptic decay constant condition, τ^d was fixed to 35 ms. For the tuned synaptic decay condition, $\tau^d_{min} = 20$ ms and $\tau^d_{max} = 50$ ms.

Fig. 6. For Fig. 6A, all 100 rate RNNs ($N = 250$, $\tau^d_{min} = 20$ ms, $\tau^d_{max} = 100$ ms) trained in Fig. 4E were converted to LIF RNNs with different values of the refractory period. The following 20 refractory period values were considered: 0, 0.5, 1.0, 1.5, 2.0, 2.5, 3.0, 3.5, 4.0, 4.5, 5.0, 10, 15, 20, 25, 30, 35, 40, 45, 50 ms.

Fig. 7. The following softplus function was used:

$$r = \log(\exp(x) + 1)$$

For the networks trained with the softplus and ReLU activation functions, the following range of values for $1/\lambda$ was used for the grid search: 4 to 26 with a step size of 2.

Quadratic integrate-and-fire model. For the quadratic integrate-and-fire (QIF) model (Fig. S7), we considered a network of units governed by

$$\tau_m \frac{d\boldsymbol{v}}{dt} = \boldsymbol{v}^2 + W^{spk}\boldsymbol{r}^{spk} + \boldsymbol{I}_{ext}$$

The definitions of the variables are identical to the ones used for the LIF network model.

Code availability. The implementation of our framework and the codes to generate all the figures in this work are available at https://github.com/rkim35/spikeRNN. The repository also contains implementation of other tasks including autonomous oscillation and exclusive OR (XOR) tasks.

Data availability. All the trained models used in the present study are available at the following repository: https://osf.io/jd4b6.

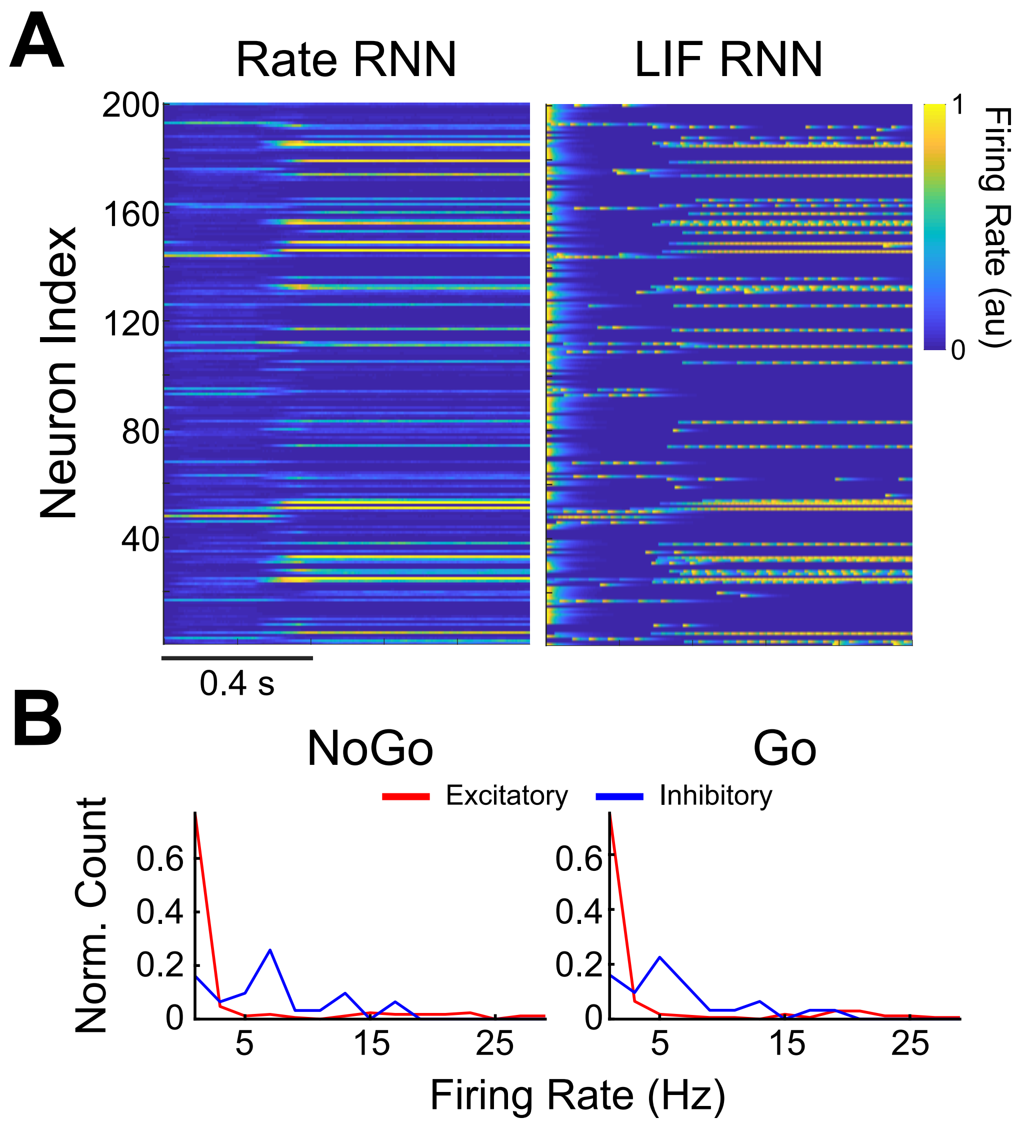

Fig. S1. Comparison of the time-varying rates of the continuous-variable rate units and the LIF units. A. A single Go trial was used to extract the rates from the rate RNN trained in Fig. 1B. The firing rates of the LIF RNN constructed using the optimal scaling factor ($\lambda = 1/25$) are shown on the right. The firing rates of the LIF units were normalized to range from 0 to 1 for comparison. **B.** Distribution of the firing rates for a NoGo trial (left) and a Go trial (right).

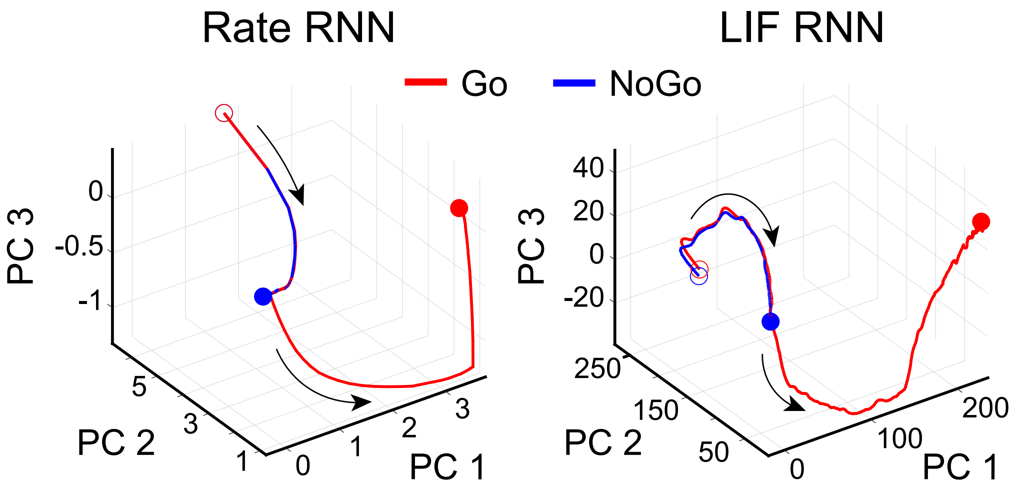

Fig. S2. Comparison of the top three PCs extracted from the network activities of the rate and LIF RNNs trained to perform the Go-NoGo task. Principal component analysis (PCA) was performed on the firing rates derived from a rate RNN and a LIF RNN trained to perform the Go-NoGo task. The rate RNN contained 200 units (169 excitatory and 31 inhibitory units), and the LIF model was constructed from the rate model. The firing rates from 50 Go trials and 50 NoGo trials were obtained from the two RNN models. For both models, the top three principal components (PCs) captured 99% of the variance. Red and blue empty circles indicate the trial onset for the Go and the NoGo trials, respectively. Red and blue filled circles represent the end of the trial for the Go and the NoGo trials, respectively.

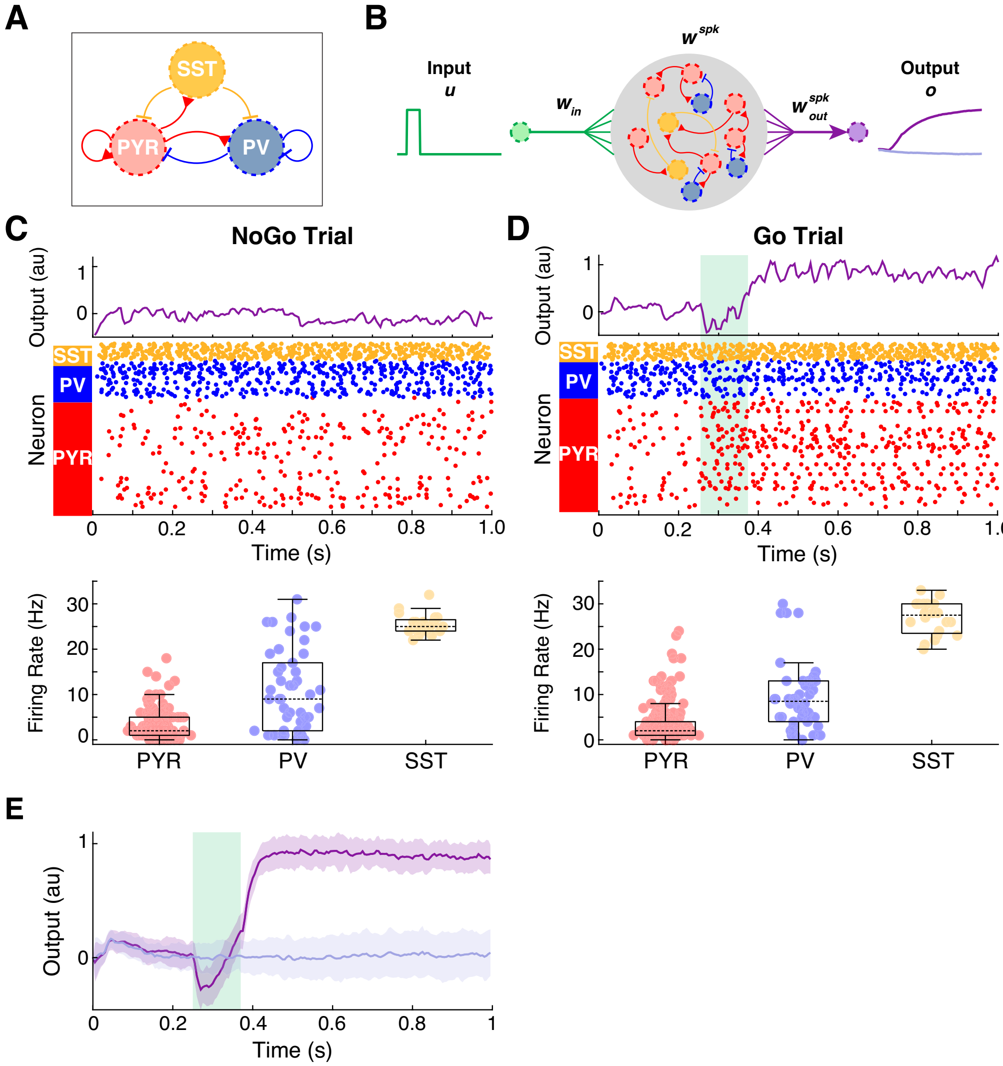

Fig. S3. Incorporation of additional functional connectivity constraints. **A.** Common cortical microcircuit motif where somatostatin-expressing interneurons (SST; yellow circle) inhibit both pyramidal (PYR; red circle) and parvalbumin-expressing (PV; blue circle) neurons. **B.** Schematic illustrating the incorporation of the connectivity motif shown in **A** into a LIF network model. The connectivity pattern was imposed during training of a rate network model ($N = 200$) to perform the Go-NoGo task. There were 134 PYR, 46 PV, and 20 SST units. A spiking model was constructed using the trained rate model with $\lambda = 1/50$. **C.** Example output response and spikes from the LIF network model for a single NoGo trial. Mean $\pm$ SD firing rate for each population is also shown (PYR, 3.08 $\pm$ 3.29 Hz; PV, 10.80 $\pm$ 8.94 Hz; SST, 25.50 $\pm$ 2.33 Hz). **D.** Example output response and spikes from the LIF network model for a single Go trial. Mean $\pm$ SD firing rate for each population is also shown (PYR, 4.72 $\pm$ 5.89 Hz; PV, 9.30 $\pm$ 8.16 Hz; SST, 27.05 $\pm$ 3.98 Hz). Box plot central lines, median; bottom and top edges, lower and upper quartiles. **E.** LIF network model performance on 50 NoGo trials (light purple) and 50 Go trials (dark purple). Mean $\pm$ SD shown.

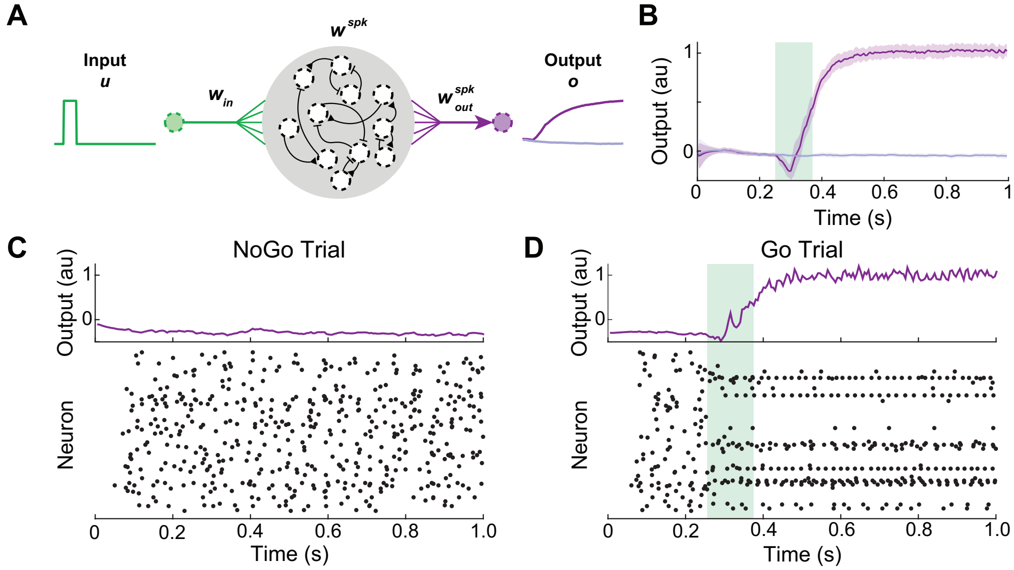

Fig. S4. Dale's principle constraint can be relaxed. A. Schematic diagram showing a LIF network model without Dale's principle. A rate RNN model ($N = 200$) without Dale's principle was first trained to perform the Go-NoGo task. The scaling factor (λ) was set to 1/50. Note that each unit (black dotted circles) can exert both excitatory and inhibitory effects. **B.** LIF network model performance on 50 NoGo trials (light purple) and 50 Go trials (dark purple). Mean $\pm$ SD shown. **C.** Example output response (top) and spikes (bottom) from the LIF network model for a single NoGo trial. **D.** Example output response (top) and spikes (bottom) from the LIF network model for a single Go trial.

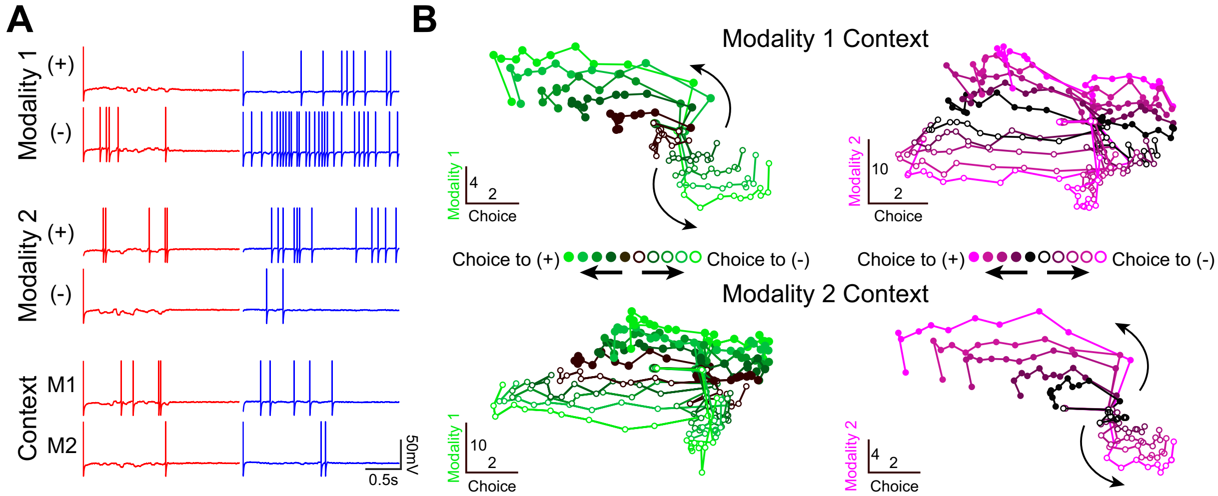

Fig. S5. The LIF network model employs mixed representations of the task variables. A. Mixed representation of the task variables at the level of single units from a LIF network ($N = 400$; 299 excitatory and 101 inhibitory units; $\tau^d_{min} = 20$ ms and $\tau^d_{max} = 100$ ms). An excitatory unit (red) and an inhibitory unit (blue) with mixed representation of three task variables (modality 1, modality 2, and context) are shown as examples. The excitatory neuron preferred modality 1 input signals with negative offset values, modality 2 signals with positive offset values, and modality 1 context (left column). The inhibitory neuron also exhibited similar biases (right column). **B.** Average population responses projected to a low dimensional state space. The targeted dimensionality reduction technique (developed in (1)) was used to project the population activities to the state space spanned by the task-related axes. For the modality 1 context (top row), the population responses from the trials with various modality 1 offset values were projected to the choice and modality 1 axes (left). The same trials were sorted by the irrelevant modality (modality 2) and shown on the right. Similar conventions used for the modality 2 context (bottom row). The offset magnitude (i.e. amount of evidence toward "+" or "-" choice) increases from dark to light. Filled and empty circles correspond to "+" choice and "-" choice trials, respectively.

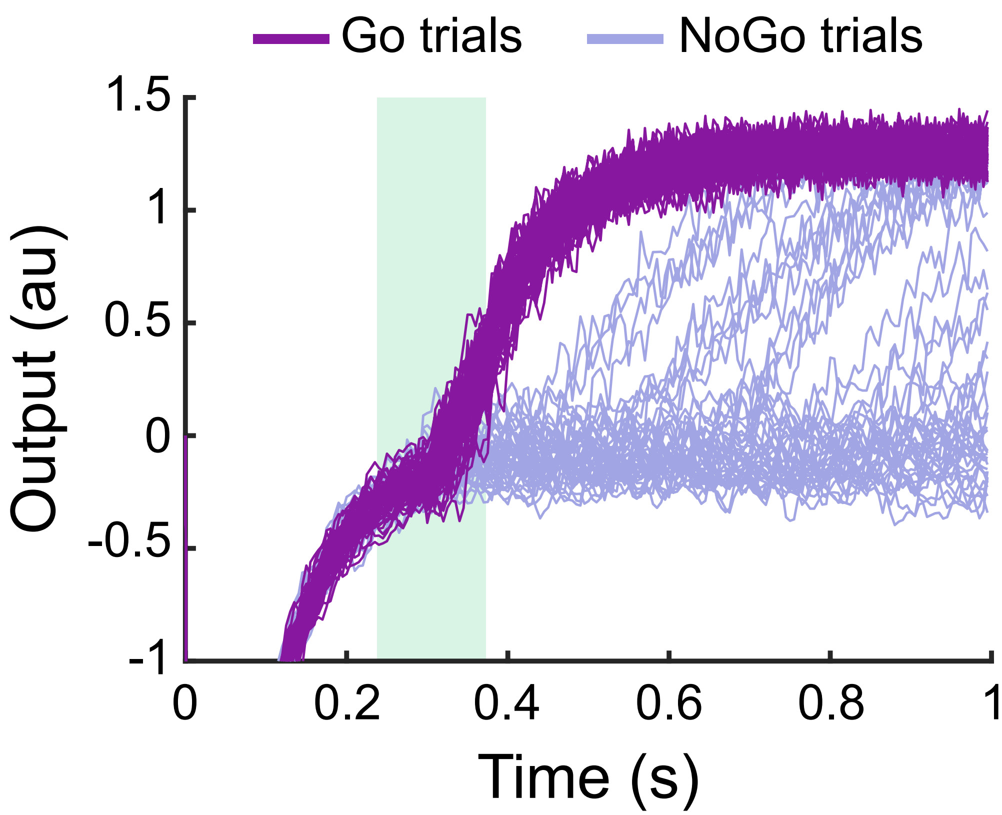

Fig. S6. **Example output responses from a softplus LIF RNN constructed to perform the Go-NoGo task.** Individual output responses from 50 Go trials (dark purple) and 50 NoGo trials (light purple) are shown. The optimal scaling factor was 1/10, and the performance of the model was 78%.

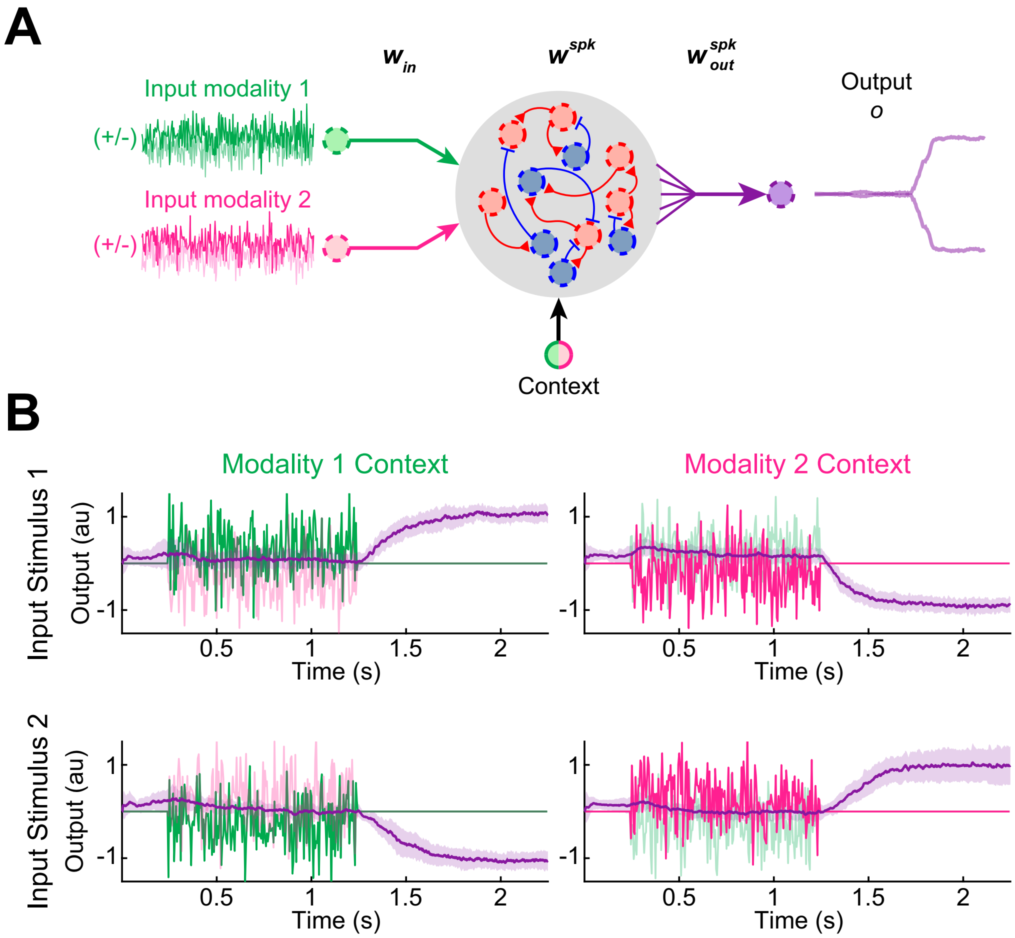

Fig. S7. **Quadratic integrate-and-fire (QIF) model constructed to perform the context-dependent input integration task.** **A.** The task paradigm and the trained rate network model used for Fig. S5 were employed to build a QIF model. The QIF model parameter values are listed in Table S1. **B.** The QIF model successfully performed the task by integrating cued modality input signals. Example noisy input signals (scaled by 0.5 vertically for visualization; green and magenta lines) from a single trial are shown. Mean $\pm$ SD response signals (purple lines) across 50 trials for each trial type.

References

1. Mante V, Sussillo D, Shenoy KV, Newsome WT (2013) Context-dependent computation by recurrent dynamics in prefrontal cortex. *Nature* 503(7474):78–84.

Table S1. Parameter values used to construct LIF and QIF networks.

	LIF	QIF
Membrane time constant (τ_m)	10 ms	10 ms
Absolute refractory period	2 ms	2 ms
Synaptic rise time (τ_r)	2 ms	2 ms
Constant bias current	-40 pA	0 pA
Spike threshold	-40 mV	30 mV
Spike reset voltage	-65 mV	-65 mV